

Figure S1

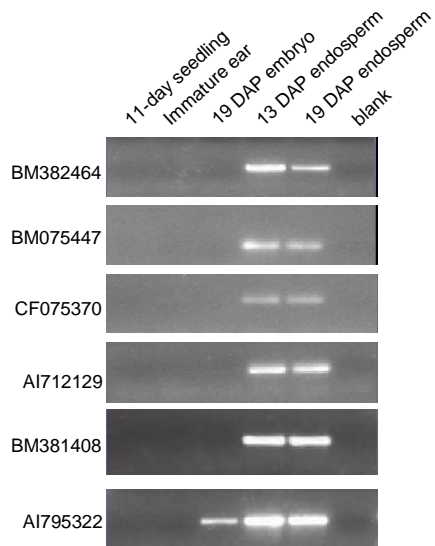
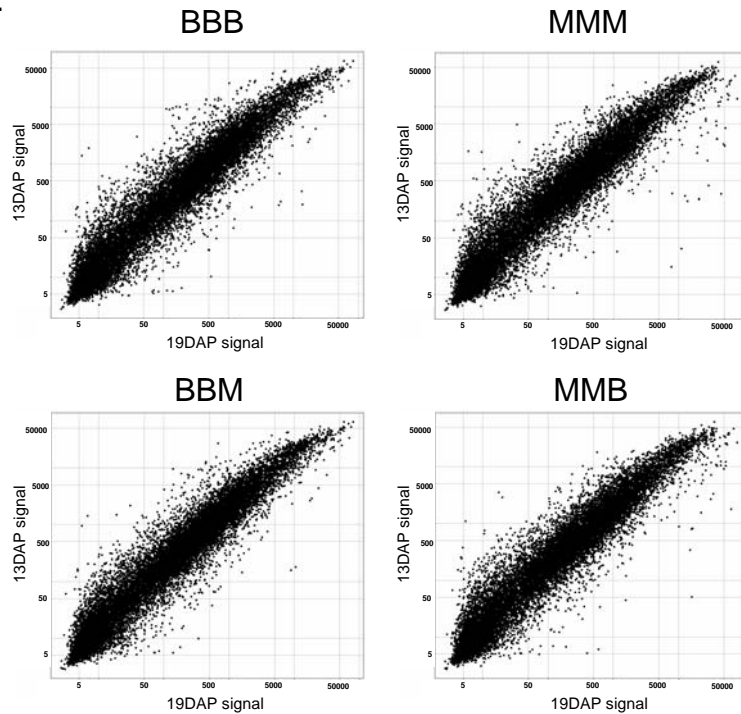


Figure S1. RT-PCR validation of endosperm-specific gene expression. RT-PCR results are shown for six of the 31 putative endosperm-specific expression patterns that we attempted to validate (Table SII). PCR was performed using cDNA derived from 13 and 19 DAP endosperm tissue as well as three vegetative tissues including 11-day seedling, immature ear and 19 DAP embryo. The “blank” lane is a no template control. Control reactions were also performed to show that we did not have genomic DNA contamination in these cDNA samples.

Figure S2.

**A**



**B**

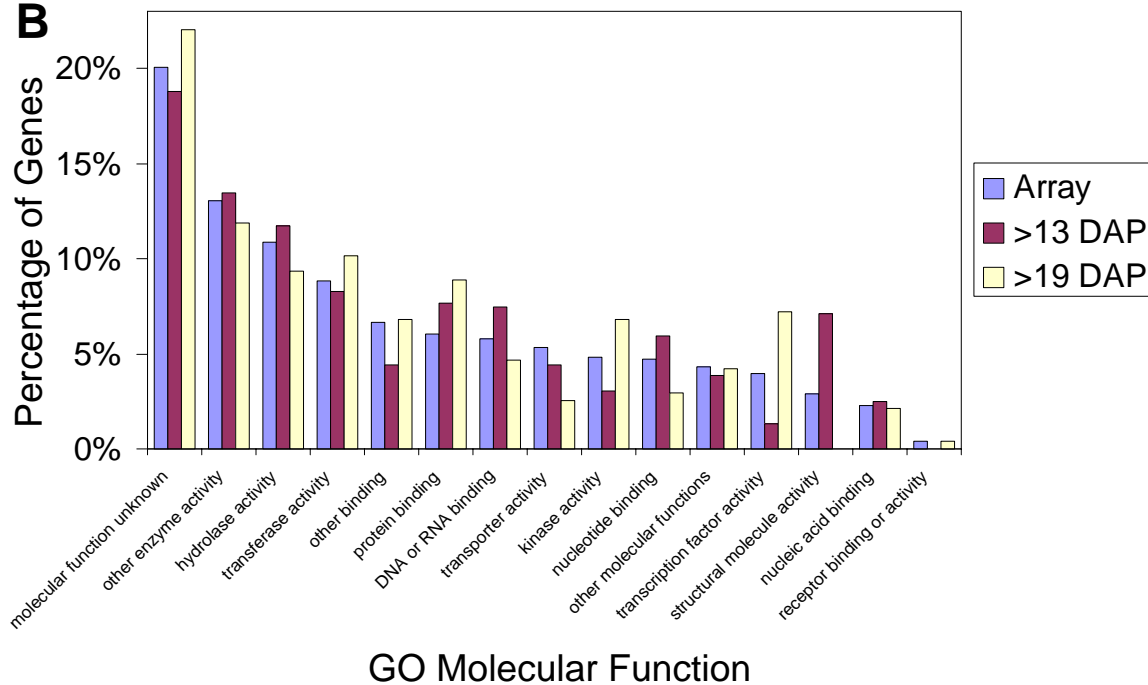
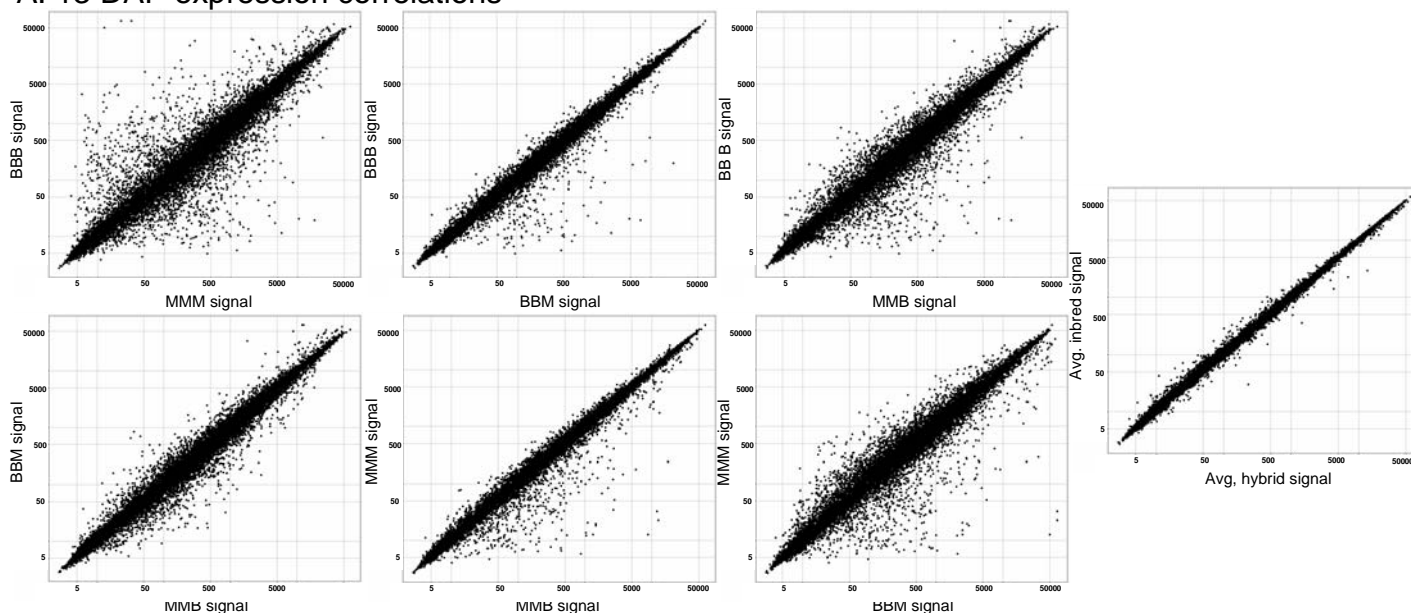


Figure S2. Comparison of endosperm gene expression at 13 and 19 DAP. (A) Correlation of microarray gene expression levels in 13 DAP and 19 DAP endosperm tissue. The log-transformed signal level in 13 DAP and 19 DAP tissue was graphed for each of the four genotypes that were analyzed. (B) The distribution of differentially expressed genes by gene ontologies for molecular function. The distribution of gene ontologies of all genes on the microarray (blue bars) is compared with the distribution of ontologies from the genes upregulated in 13 DAP endosperm (red bars) or in 19 DAP endosperm (yellow bars). The GO terms are ordered on the graph from highest frequency on the array (left) to lowest frequency on the array (right).

Figure S3

A. 13 DAP expression correlations



B. 19 DAP expression correlations

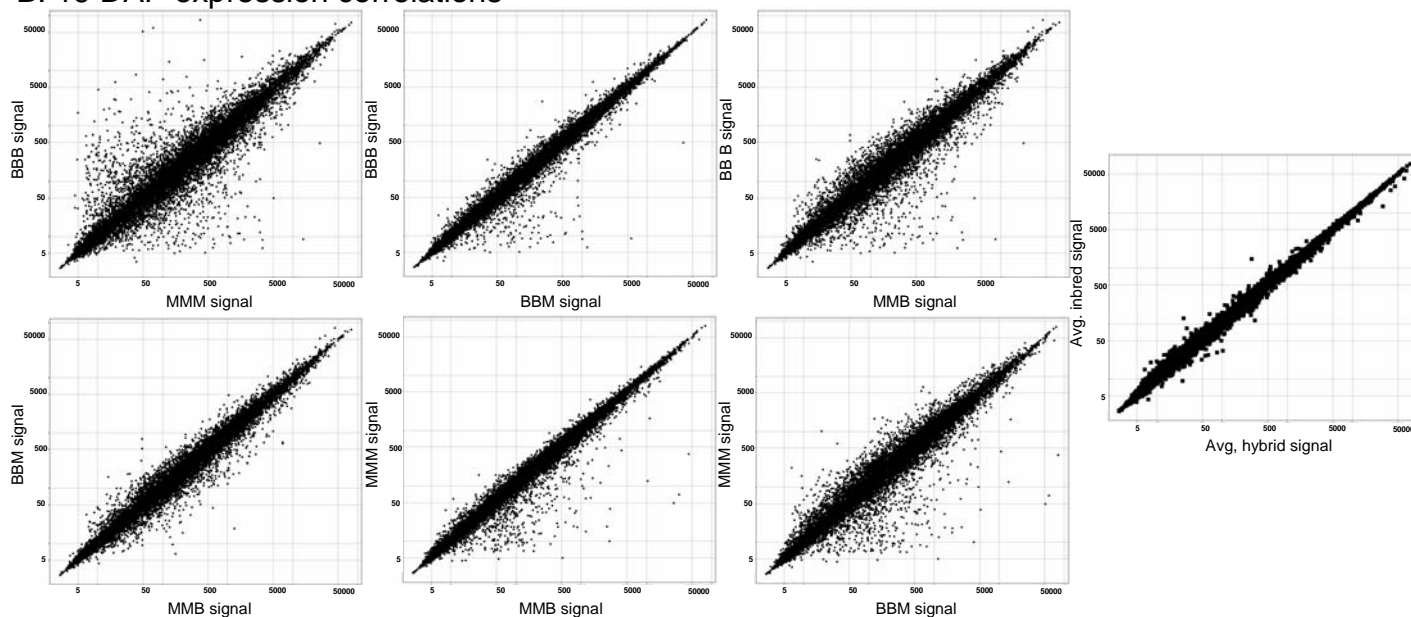
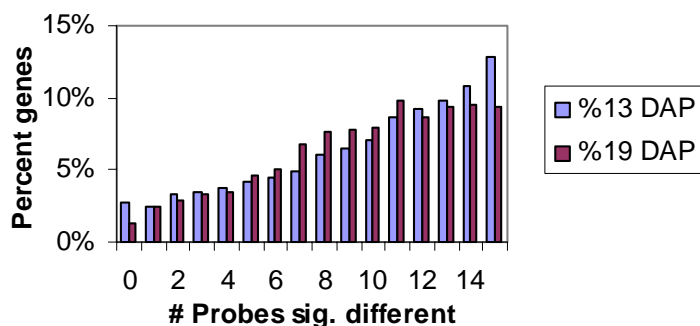


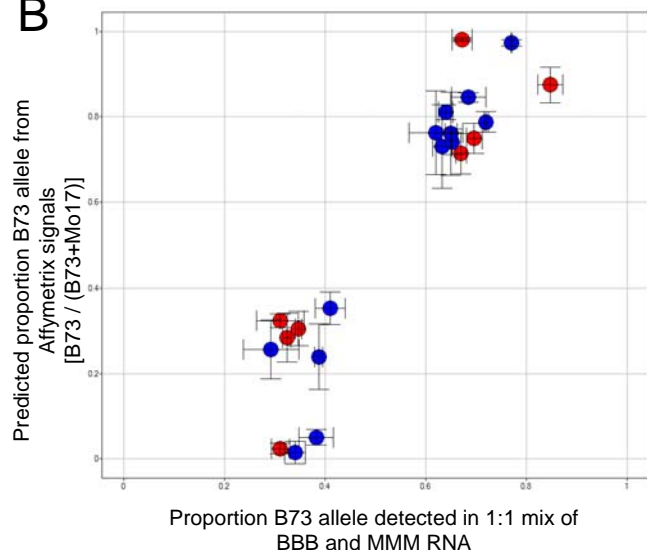
Figure S3. Genotype affects on gene expression (A) Genotype affects on gene expression in 13 DAP endosperm are visualized using log-scale correlation plots to compare the signal for different genotypes in 13 DAP endosperm tissue. (B) Genotype affects on gene expression in 19 DAP endosperm are similarly displaying using log-scale correlation plots.

Figure S4

**A Probe level support of differential expression**



**B**



**C**

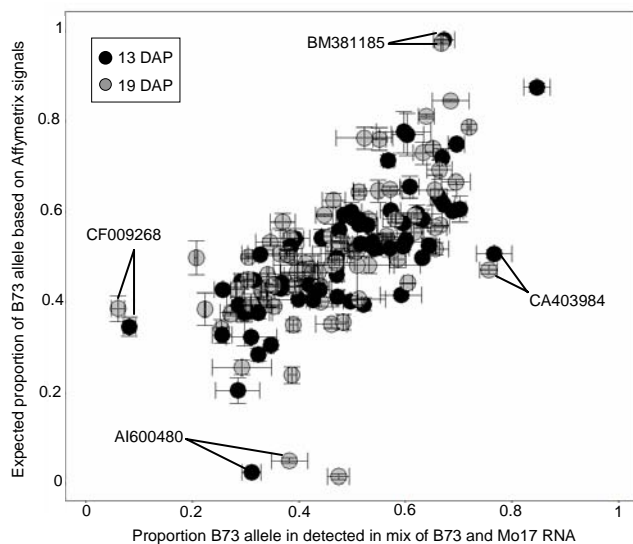


Figure S4. Validation of microarray data. A) A microarray probe level analysis was performed to assess the potential affects of sequence polymorphisms on the ability for two alleles to be detected by the Affymetrix microarray. A t-test was performed to compare the three biological replicates of B73 to the three biological replicates for Mo17 for each of the 15 perfect match probes for each differentially expressed gene. The number of probes that were significantly different in B73 and Mo17 ( $p=0.05$ ) were determined for each gene. The graph indicates the percent of genes with each number of significant probes. Eight or more of the probes were significantly different in B73 and Mo17 for the majority of genes. B) For the subset of genes that were called differentially expressed in the Affymetrix analysis and had available allele-specific expression data we determined the correlation between the predicted relative expression of B73 based on Affymetrix microarray data [B73 signal divided by (B73 + Mo17 signal)] and the relative fraction of B73 allele present in a 1:1 mix of BBB and MMM inbred RNAs validates the microarray differential expression calls and directionality. (C) The correlation between the allele-specific expression data and microarray data is presented for the 81 genes in which allele-specific expression and microarray data were available. For each gene we plotted the average proportion of the B73 allele that was detected in B73-Mo17 mixes of RNA from 13 DAP (black) or 19 DAP (gray) on the y-axis. The x-axis is computed from Affymetrix microarray signal values from arrays hybridized with B73 or Mo17 RNA. The values is derived using the following formula:  $(B73 \text{ signal}) / (B73 \text{ signal} + Mo17 \text{ signal})$ . We have indicated the accession numbers of four genes that showed significant deviation between microarray and allele-specific expression data.

Figure S5

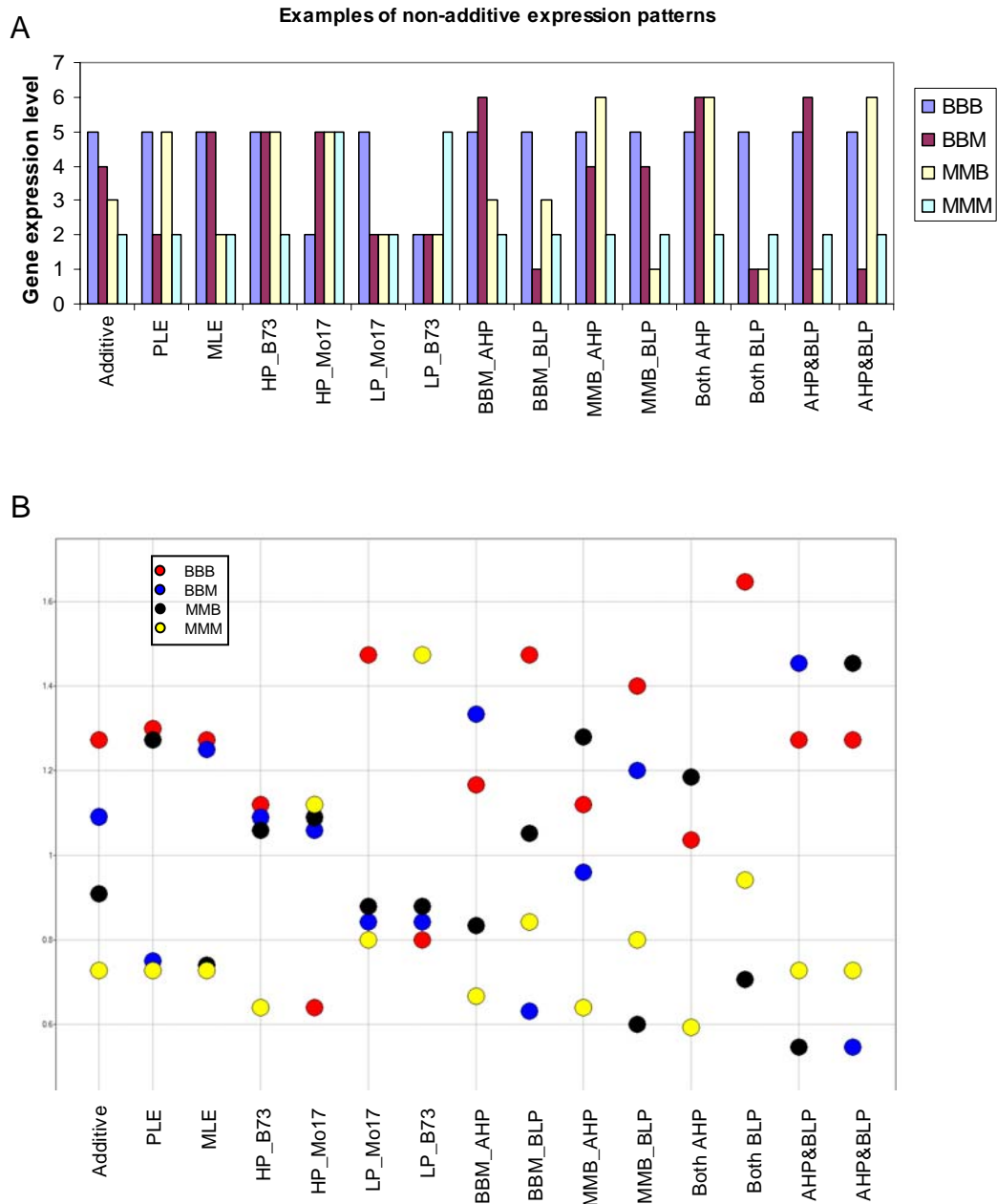


Figure S5. Examples of the expression patterns that would be expected for the additive and non-additive expression classes. (A). Sample expression values are plotted for examples of the fifteen classes of potential gene expression pattern. (B) For the fifteen example “genes” the hypothetical microarray signal (normalized to an value of 1 for each gene) for each of the four genotypes is plotted along the vertical axis. This format is applied to real data in Figures S6-S12.

Figure S6

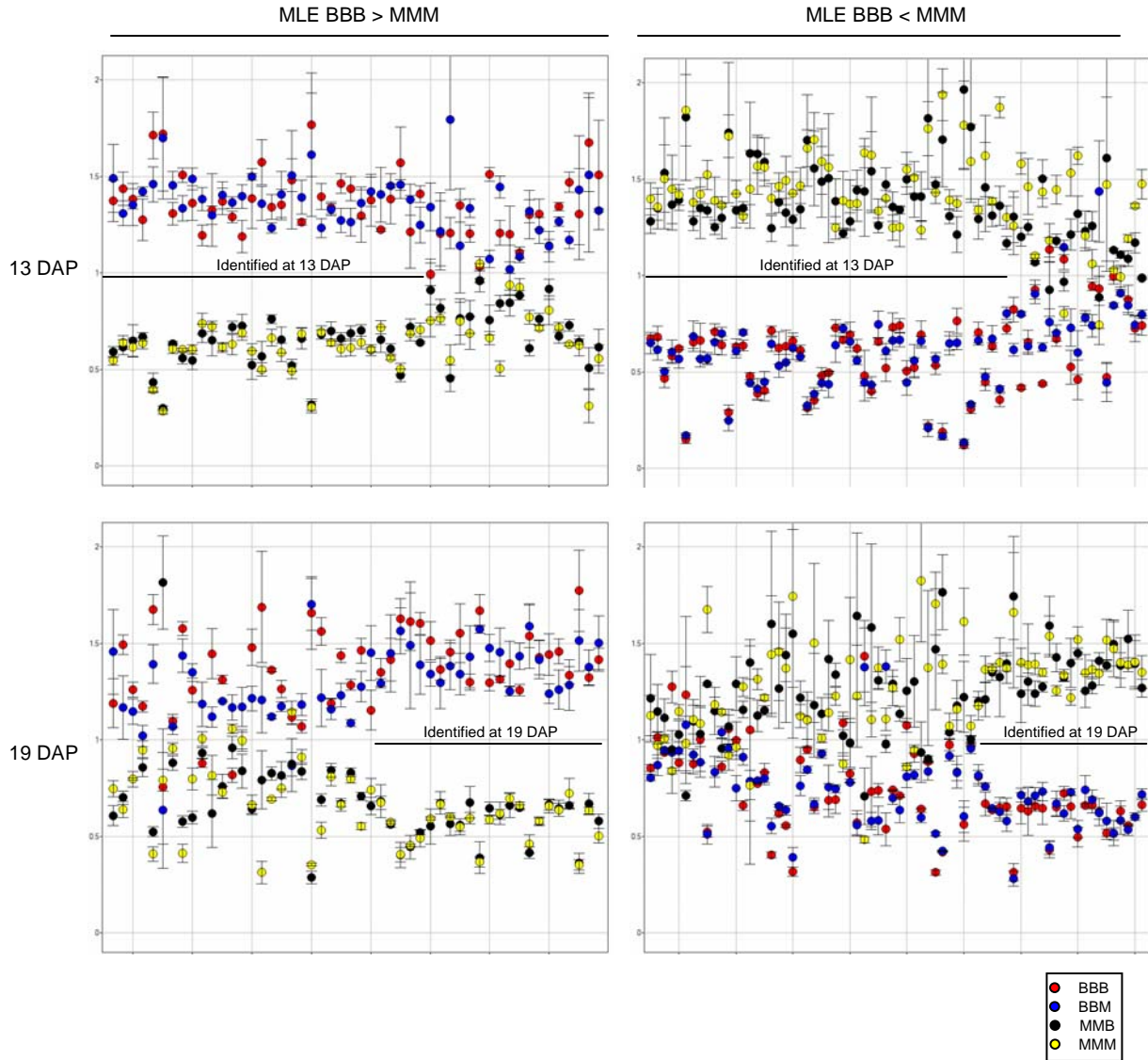


Figure S6. Expression plots for genes that display MLE patterns in the microarray data. A total of 120 genes with MLE patterns were identified in either 13 or 19 DAP endosperm tissue. In (A) the relative expression for the four genotypes in 13 DAP endosperm is displayed while (B) displays the relative expression in 19 DAP endosperm. The black bars indicate which tissues the statistically significant MLE pattern was observed for. Note that for six genes MLE patterns were identified in both 13 and 19 DAP endosperm. For 53 of the 81 genes that were identified as having MLE patterns in 13 DAP endosperm we also observed maternal-like patterns in 19 DAP endosperm tissue. Similarly, for 29 of the 44 genes identified as MLE in 19 DAP endosperm also displayed maternal-like patterns in 13 DAP endosperm.

Figure S7

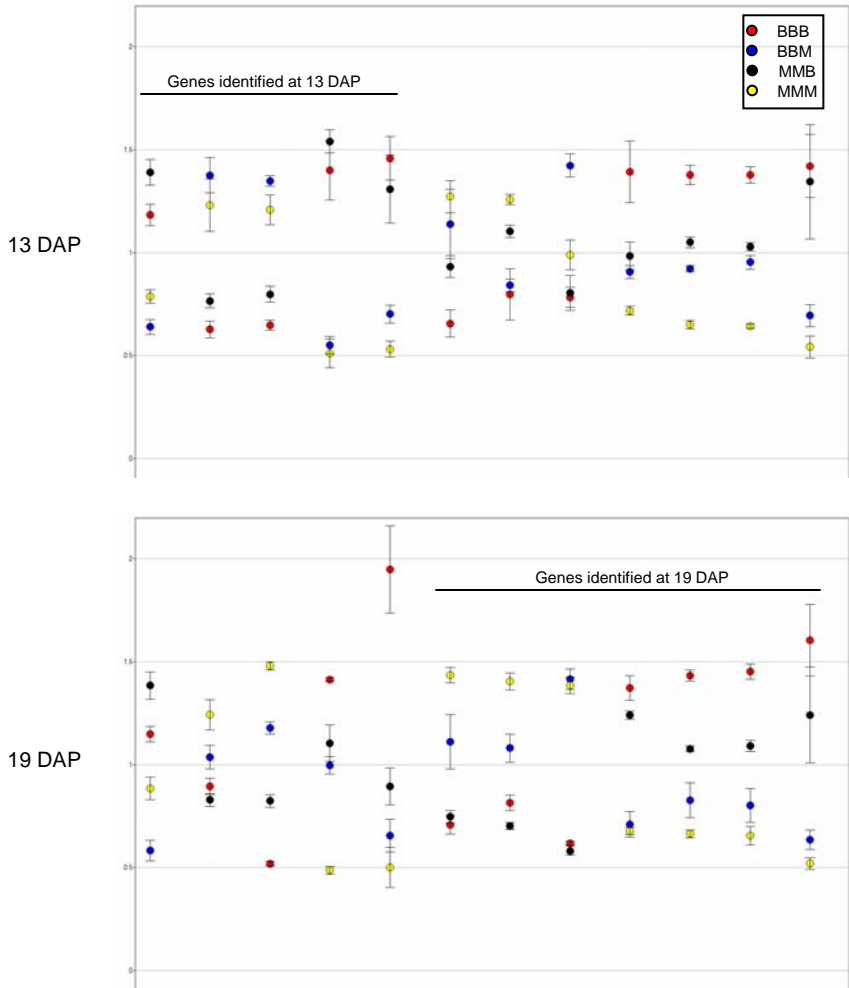


Figure S7. Expression plots for genes that display PLE patterns. A total of 12 genes that displayed PLE patterns were identified in our analysis. In both plots the first five genes were identified based on their expression in 13 DAP endosperm while the next seven genes were identified based on their expression in 19 DAP endosperm. The normalized expression levels for the four genotypes were graphed in 13 DAP (upper graph) and in 19 DAP endosperm (lower graph). For each gene the expression values for the four genotypes are displayed along the vertical axis with the standard deviations indicated by black lines. Note that for all five of the PLE genes identified at 13 DAP the expression pattern in 19 DAP endosperm is also paternal-like and 6/7 PLE genes identified in 19 DAP endosperm also show paternal-like expression in 13 DAP endosperm.



Figure S8

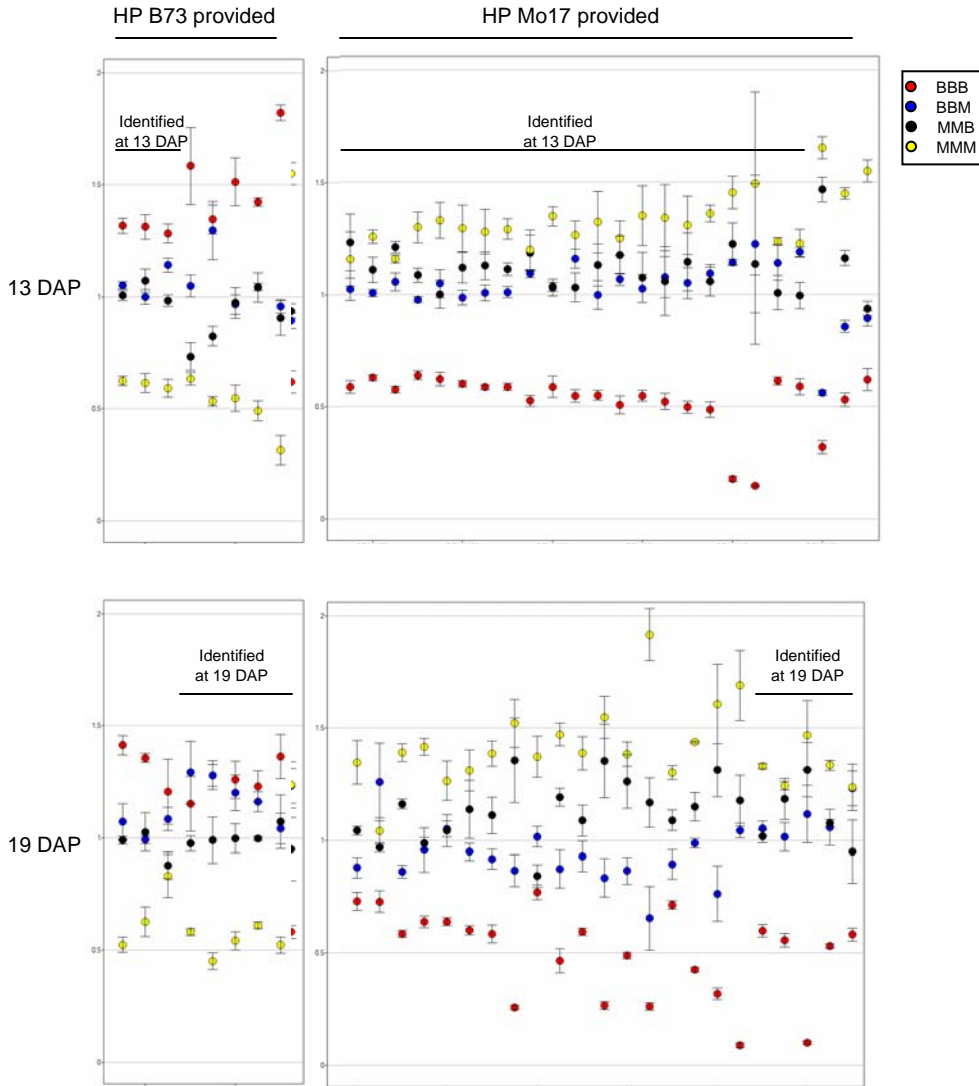


Figure S8. Expression plots for genes that display high parent (HP) patterns. All of the genes that display HP patterns in which the dominant *trans*-acting locus is provided by B73 (8 genes) or Mo17 (24 genes) were identified. The tissue in which the statistically significant pattern was discovered is noted by the black lines in the graphs (note that two of the HP Mo17 genes were identified in both 13 and 19 DAP). For half of the HP genes (15/32), both 13 and 19 DAP tissues display HP-like patterns.



Figure S9

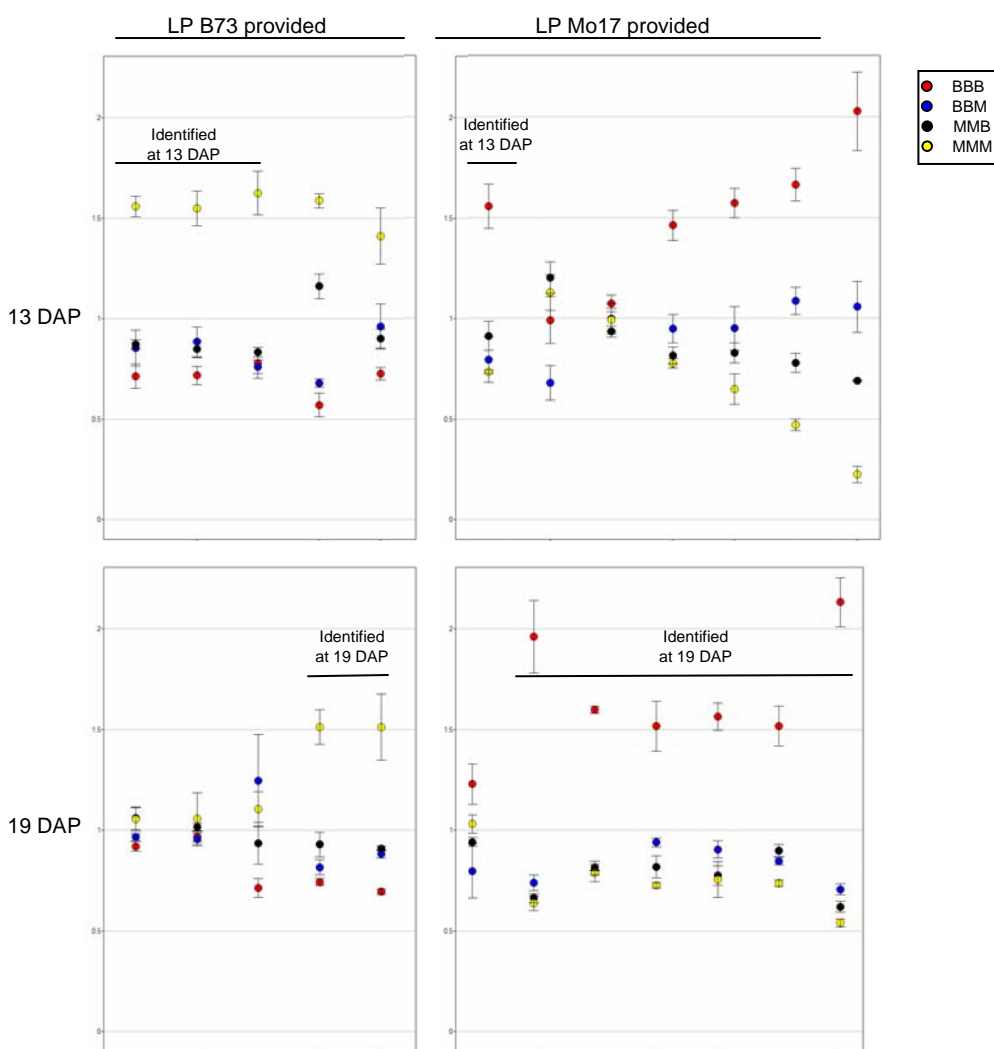


Figure S9. Expression plots for genes that display low parent (LP) patterns. All of the genes that display LP patterns in which the dominant *trans*-acting locus is provided by B73 (5 genes) or Mo17 (7 genes) were identified. The tissue in which the statistically significant pattern was discovered is noted by the black lines in the graphs. For half of the LP genes (6/12), both 13 and 19 DAP tissues display LP-like patterns.

Figure S10

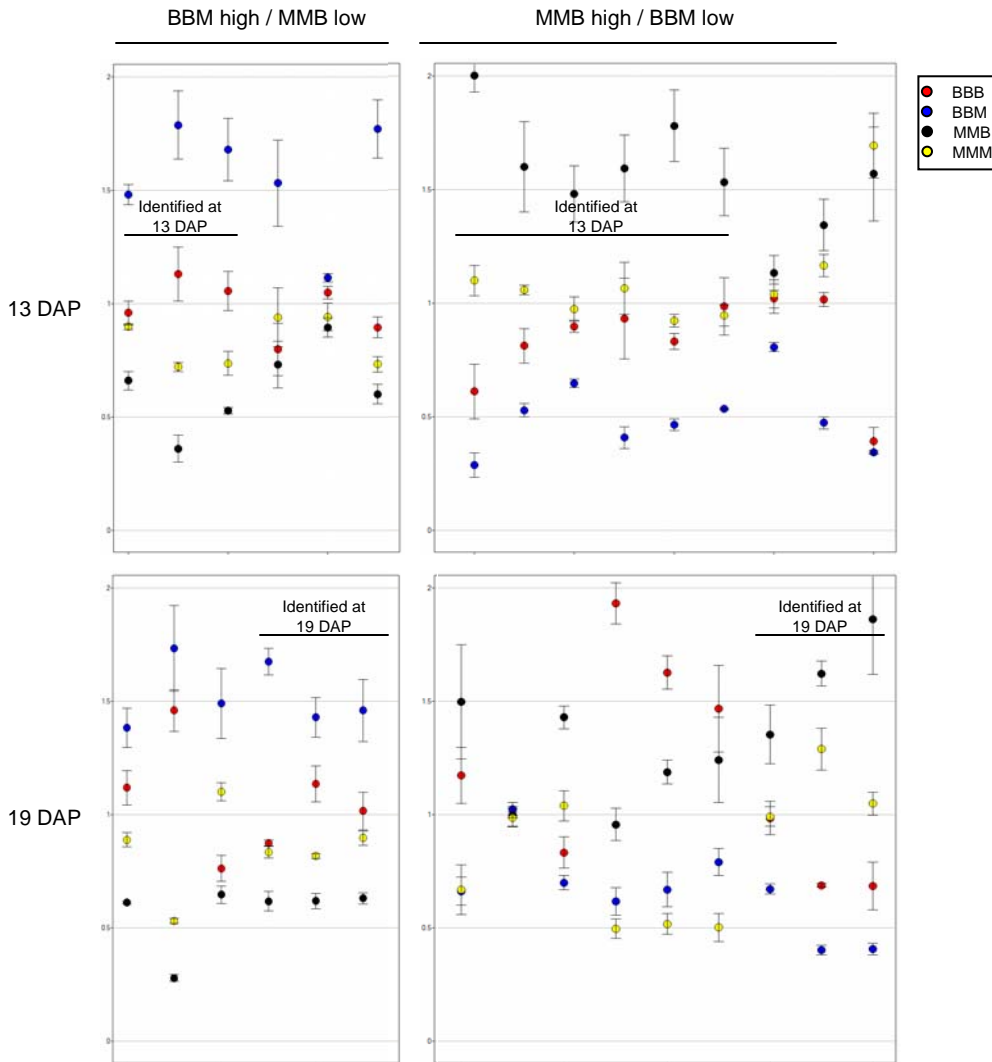


Figure S10. Expression plots for genes that display expression patterns in which one hybrid is above the range of the parents and the other hybrid is below the range of the parents. A set of six genes were identified for which B73 x Mo17 (BBM) hybrids displayed expression levels above the range of the parent while the reciprocal hybrid Mo17 x B73 (MMB) was expressed below the range of the parents. Nine genes that displayed above high parent expression of MMB and below low parent expression of BBM were also identified. These plots allow analysis of the expression levels for these genes in both 13 and 19 DAP tissues. Note that 9/16 genes show expression of the hybrids outside the range of the parents for both time points.

Figure S11

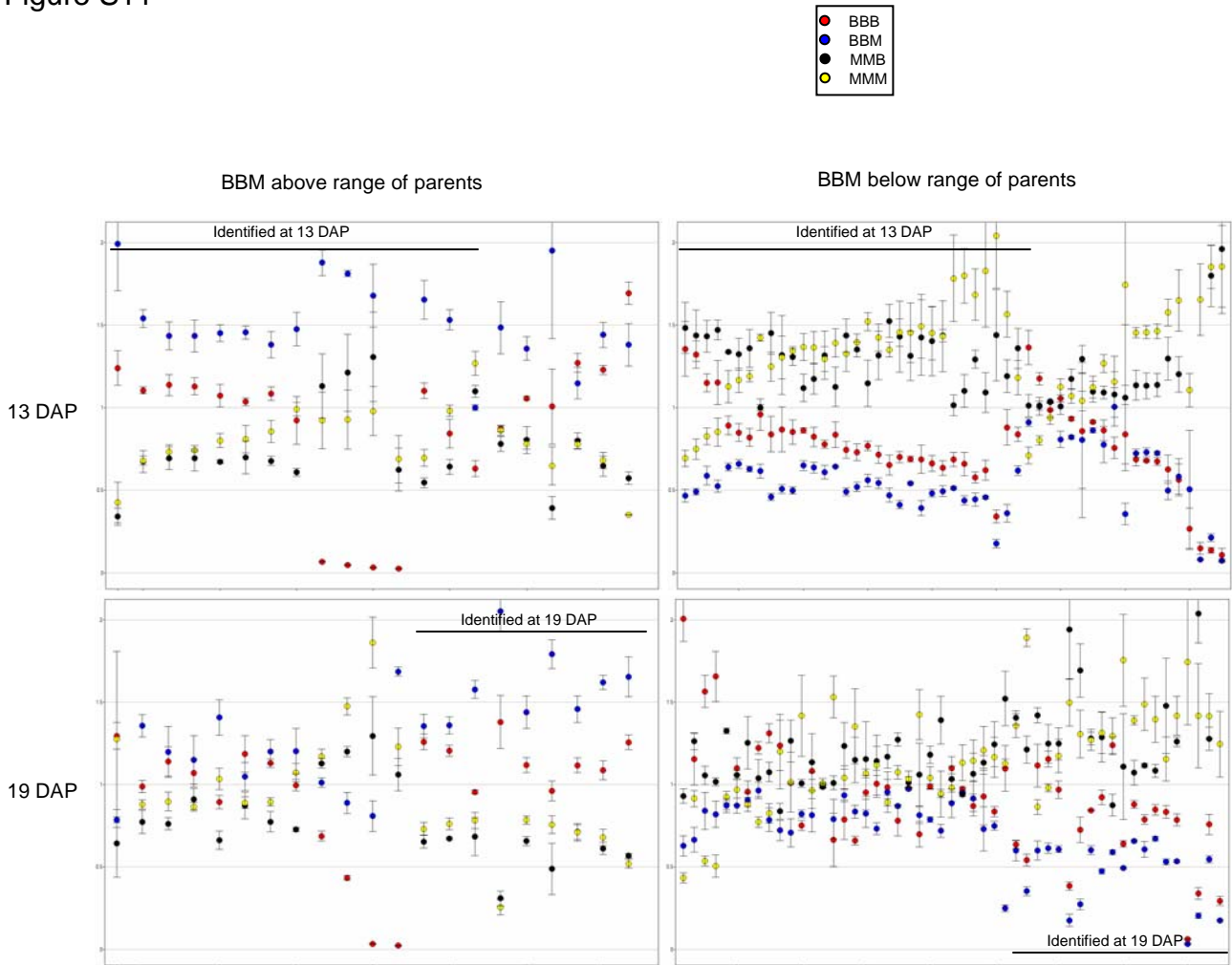


Figure S11. Expression plots for genes that display expression patterns in the B73 x Mo17 (BBM) hybrid outside the range of the parents. The upper graphs show the relative expression in 13 DAP endosperm while the lower graphs display the relative expression in 19 DAP endosperm. The graphs on the left display the expression levels for the 21 genes that display BBM above-high parent expression while the graphs on the right display the expression levels for the 51 genes that display BBM below-low parent expression. The black bars indicate the tissue in which the statistically significant expression pattern was identified. Note that for both above-high parent and below-low parent patterns there were two genes that were identified in both 13 and 19 DAP endosperm tissue. 14/21 genes that display above-high parent expression showed similar expression patterns at both 13 and 19 DAP endosperm. 24/51 genes that display below-low parent expression showed similar expression patterns at both time points.

Figure S12

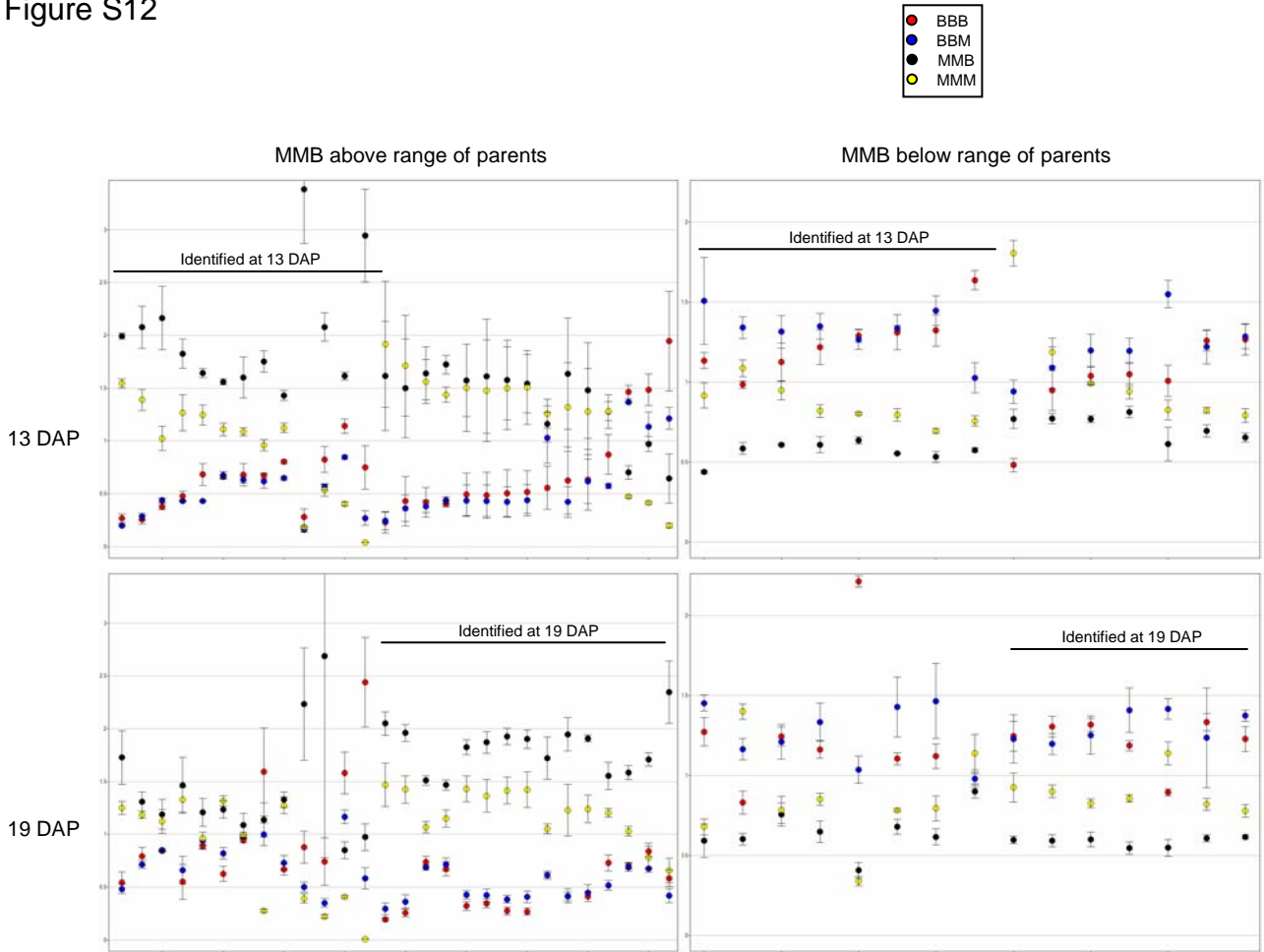


Figure S12. Expression plots for genes that display expression patterns in the Mo17 x B73 (MMB) hybrid outside the range of the parents. The upper graphs show the relative expression in 13 DAP endosperm while lower graphs display the relative expression in 19 DAP endosperm. The graphs on the left display the expression levels for the 28 genes that display MMB above-high parent expression while the graphs on the right display the expression levels for the 15 genes that display MMB below-low parent expression. The black bars indicate the tissue in which the statistically significant pattern was identified. Note that for both above-high parent and below-low parent patterns there were two genes that were identified in both 13 and 19 DAP endosperm tissue. 17/28 genes that display above-high parent expression showed similar expression patterns at both 13 and 19 DAP endosperm. 13/15 genes that display below-low parent expression showed similar expression patterns at both time points.

Figure S13

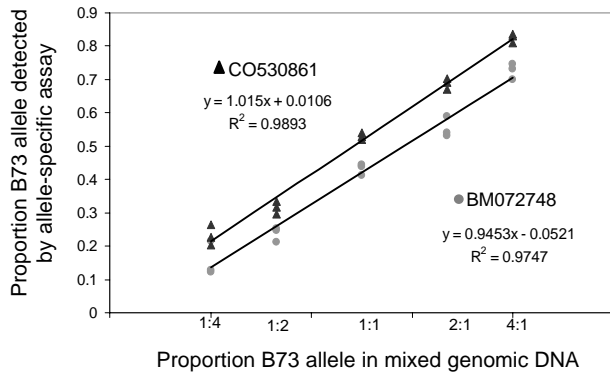


Figure S13. Calibration of allele-specific expression assays. Each SNP assay was performed on three replicates of DNA mixes. The B73 and Mo17 DNA was mixed in ratios of 1:4, 1:2, 1:1, 2:1 and 4:1. The data is shown for assays that detect SNPs in the genes CO530861 and BM072748. From this data we can produce an equation that will correct for slight biases in the assays to predict the proportion of the B73 allele in any sample.